ACS Catalysis

Research Article

Cite This: ACS Catal. 2019, 9, 315−324

pubs.acs.org/acscatalysis

Dimerization of Linear Butenes on Zeolite-Supported Ni^{2+}

Andreas Ehrmaier,[†] Yue Liu,[†] Stephan Peitz,[‡] Andreas Jentys,[†] Ya-Huei Cathy Chin,[†,§] Maricruz Sanchez-Sanchez,*[,†] Ricardo Bermejo-Deval,*[,†] and Johannes Lercher*[,†,∥]

[†]Department of Chemistry and Catalysis Research Center, Technische Universität München, Lichtenbergstrasse 4, D-85747 Garching, Germany

[‡]Evonik Performance Materials GmbH, 45772 Marl, Germany

[§]Department of Chemical Engineering and Applied Chemistry, University of Toronto, Toronto, Ontario M5S 3E5, Canada

[∥]Institute for Integrated Catalysis, Pacific Northwest National Laboratory, P.O. Box 999, Richland, Washington 99352, United States

Supporting Information

ABSTRACT: Nickel- and alkali-earth-modified LTA based zeolites catalyze the dimerization of 1-butene in the absence of Brønsted acid sites. The catalyst reaches over 95% selectivity to *n*-octenes and methylheptenes. The ratio of these two dimers is markedly influenced by the parallel isomerization of 1-butene to 2-butene, shifting the methylheptene/octene ratio from 0.7 to 1.4 as the conversion increases to 35%. At this conversion, the thermodynamic equilibrium of 90% *cis*- and *trans*-2-butenes is reached. Conversion of 2-butene results in methylheptene and dimethylhexene with rates that are 1 order of magnitude lower than those with 1-butene. The catalyst is deactivated rapidly by strongly adsorbed products in the presence of 2-butene. The presence of π-allyl-bound butene and Ni-alkyl intermediates was observed by IR spectroscopy, suggesting both to be reaction intermediates in isomerization and dimerization. Product distribution and apparent activation barriers suggest 1-butene dimerization to occur via a 1′-adsorption of the first butene molecule and a subsequent 1′- or 2′-insertion of the second butene to form octene and methylheptene, respectively. The reaction order of 2 for 1-butene and its high surface coverage suggest that the rate-determining step involves two weakly adsorbed butene molecules in addition to the more strongly held butene.

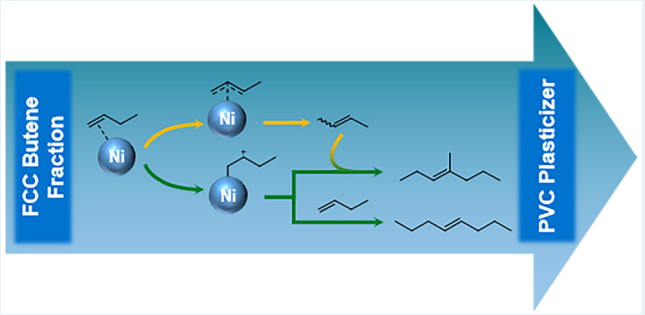

KEYWORDS: *linear alkenes, nickel Lewis acid zeolite, dimerization, nickel alkyl and LTA zeolite*

INTRODUCTION

Linear and single-branched alkenes and in particular octenes are important intermediates in the synthesis of high-value products, such as comonomers for low-density polyethene.[1] The pathway to produce these molecules via dimerization is attractive, because it utilizes abundantly present light olefins. Nickel-based catalysts have been identified as the most promising family of catalytic materials, exhibiting a high activity and selectivity to linear alkenes.[2−7] These catalysts favor the formation of dimers and limit successive C−C bond formation.

Mechanistically, α-alkene formation has been reported to occur via a Ni-alkyl complex, following the Cossee−Arlman mechanism, a metallacycle route, and proton-transfer mechanisms.[8−10] Catalysts based on Ni dispersed on solid supports, including molecular organic frameworks, were proposed to follow the first mechanism.[6,11−19]

Indeed, ethene oligomerization over Ni-exchanged zeolites has been proposed to proceed via formation of a 1′-alkyl carbenium ion followed by a migratory insertion, while the products desorb with a β-hydride elimination (Cossee−Arlman mechanism).[20] It has been suggested that the density of liquidlike ethene is required to aid the desorption of butene, limiting C_4 isomerization and further polymerization via ethene addition.[21]

To achieve high rates and to avoid side reactions, Ni^{2+} cations have to be well separated and the support should be free of other strong acid sites, in particular Brønsted acid sites (BAS). Mesoporous and microporous crystalline aluminosilicates and amorphous aluminosilicates are supports that can potentially achieve such high Ni dispersion,[22−29] provided that two Si-O-Al exchange sites are sufficiently close to stabilize a Ni^{2+} cation. Indeed, zeolites with high framework Al concentrations (Si/Al ≈ 1−3) have been shown to be well suited. However, ion exchange with Ni^{2+} still leads frequently to isolated BAS that catalyze alkene dimerization to dimethylhexene but also lead to isomerization, oligomerization, and cracking.[30−33]

Received: August 3, 2018
Revised: November 27, 2018
Published: November 29, 2018

DOI: 10.1021/acscatal.8b03095
ACS Catal. 2019, 9, 315−324

The importance of avoiding isomerization is best illustrated with the fact that an additional pathway to branched alkenes is available for isomers with internal C=C bonds.[13,15] In the case of dimerization of butenes, isomerization of 1-butene to 2-butene opens this pathway to undesired products.[34] Therefore, minimizing the relative rate of double-bond isomerization is a critical challenge for dimerization of alkenes with more than three carbon atoms. Indeed, it is essential to combine a high concentration of isolated Ni^{2+} with the absence of BAS in order to achieve high selectivity to linear and single-branched alkenes. We have addressed this by choosing an LTA zeolite to host the Ni^{2+}, adjusting the other exchange cations not only to minimize or eliminate the presence of Brønsted acid sites but also to adjust the electronic state of Ni^{2+}.

The present paper explores Ni^{2+} exchanged Ca-LTA for butene dimerization. The narrow pores of LTA allow only the conversion at the pore mouth or on the outer surface. The rates of dimerization and competing isomerization are studied in the absence of BAS, combining the characterization of adsorbed species by IR spectroscopy and kinetic measurements. This study shows a unique chemical environment for Ni^{2+}, weakening its Lewis acidity by coadsorption of a third butene molecule.

RESULTS AND DISCUSSION

1-Butene Dimerization on Ni-Ca-LTA Catalysts. At the start, a series of Ni-Ca-LTA-based catalysts with different Ni loadings was prepared and characterized with respect to morphology and crystallinity in order to select an adequate catalyst for mechanistic studies. Details are provided in the Supporting Information. Broadening of the XRD diffraction bands of LTA was observed with increasing Ni loadings (see Figure S1 in the Supporting Information), indicating a certain loss of crystallinity due to the ion exchange.[35,36] While a hysteresis for the N_2 sorption was not observed for Ca-LTA (Figure S2), the sorption volume of the Ni-containing catalysts showed important differences during adsorption and desorption, pointing to an increase in the mesopore volume and a decrease in the micropore volume (Table S1). To minimize the effect of local lattice destruction, the loading of Ni was limited to 6 wt % on Ni-Ca-LTA. Changes in the particle size were not observed by SEM (Figure S3 and Table S2).

Analysis by X-ray absorption spectroscopy (XAS) was used to establish the oxidation state of the Ni in Ni-Ca-LTA in contact with 1-butene. Variations in the Ni-K edge energy (8333 eV) prior to and after exposure to 1-butene were not observed in the X-ray absorption near-edge structure (XANES). This indicates that Ni is present as Ni^{2+} in the acting catalyst (Figure S4A), and we conclude that Ni^{2+} is the active center for dimerization.[11,37,38]

The weight-based rate of 1-butene dimerization was determined for catalysts containing 2–6% Ni (Figure S5 and Table S3). The rate of dimerization increased linearly with the Ni concentration. This led us to conclude, in turn, that all (or a constant fraction) of Ni^{2+} is accessible to the reactants at this level of ion exchange. Therefore, detailed mechanistic studies were performed on a 6 wt % Ni exchanged Ni-Ca-LTA catalyst.

The butene conversion rates and product rate distribution upon time on stream for a 6 wt % Ni exchanged Ca-LTA are shown in Figure 1. Rates in butene conversion were the highest within the first 5 h (1.5×10^{-4} $mol_C/(g\ s)$). These rates were less than 1 order of magnitude lower than rates reported for

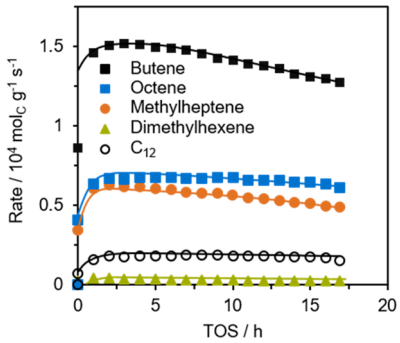

Figure 1. Reaction of 1-butene over 6 wt % Ni-Ca-LTA: butene consumption rate (black squares) and formation rates of dimerization products over time on stream with respect to moles of carbon. Conditions: T = 160 °C, p = 50 bar, WHSV = 38 h^{-1}.

zeolites and mesoporous aluminosilicates with BAS.[11,25−27] Subsequently, slight deactivation was observed with time on stream. For the mechanistic and kinetic studies in this work, the reported activity data were extrapolated to zero time on stream (TOS). Rates to octene and methylheptene were comparable ($(6–7) \times 10^{-5}$ $mol_C/(g\ s)$), while rates to dimethylhexene were of 1 order of magnitude lower. To compare the intrinsic dimerization and trimerization activities of Ni-Ca-LTA, we assumed an overall second-order reaction for each pathway: i.e., second order in butene for dimerization and first order in both butene and octene for trimerization. A higher apparent second reaction order constant was observed for trimerization ($k_{tri} = 5.67 \times 10^{-9}$ $mol_C/(g\ s\ bar^2)$) than for dimerization ($k_{di} = 1.67 \times 10^{-9}$ $mol_C/(g\ s\ bar^2)$). Thus, Ni-Ca-LTA has a higher selectivity for trimers than for dimers in the oligomerization of 1-butene. This selectivity is higher than that observed for Ni-aluminosilicates in the presence of BAS.[26] Note that an operating temperature below 200 °C prevented cracking of 1-butene and products, as was observed with similar catalysts.[25]

Product Distribution with Ni-Ca-LTA Catalysts. The oligomerization of 1-butene on a 6 wt % Ni containing LTA catalyst was conducted at 50 bar, 160 °C, and space velocities ranging from 6 to 244 h^{-1} (Figure 2). The results show higher than 80% selectivity toward octenes, with less than 20% of higher oligomers—mostly trimers (not shown). Within the dimer fraction, the main products were 3-methylheptenes and *n*-octenes (Figures 1 and 2 A). Only small amounts (less than 5% among the dimers) of 3,4-dimethylhexenes were formed. The thermodynamic dimer equilibrium under the given conditions predicts a dimethylhexene/methylheptene/octene ratio of 34/60/6 (Figure S6 in the Supporting Information): i.e., the products observed are quite distant from equilibrium.

The 1-butene consumption rate with varying space time is shown in Figure 2A. Upon higher space times, 1-butene consumption leveled off at a rate of 5×10^{-5} $mol_C/(g\ s)$, corresponding to ca. 35% conversion. It was not possible to surpass this level of conversion by an increase in space time. However, this value is far from the dimerization thermodynamic equilibrium (close to 100% 1-butene conversion as shown in Figure S6 in the Supporting Information). As the conversion increased, 1-butene was isomerized to 2-butene, reaching the thermodynamic equilibrium (Figure 3A) at the point (Figure 2A) when the 1-butene conversion rate in dimerization leveled off, at approximately 5×10^{-5} $mol_C/(g\ s)$ (conversion values of ∼30−35%, gray bar in Figure 3A).

DOI: 10.1021/acscatal.8b03095
ACS Catal. 2019, 9, 315−324

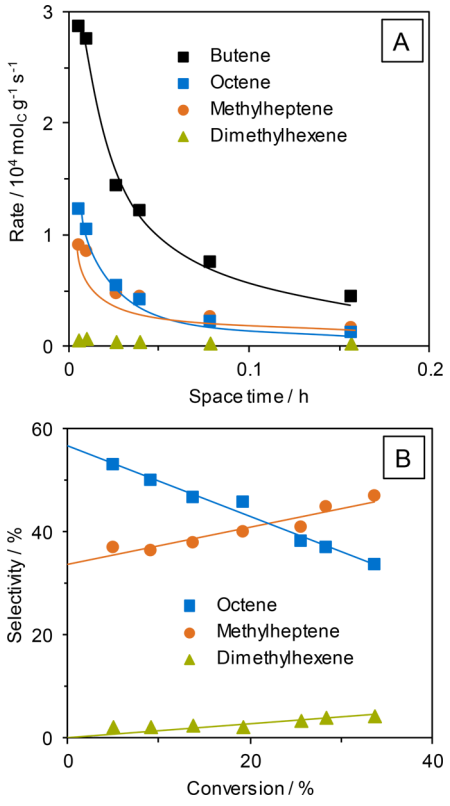

Figure 2. (A) Effect of space time on the catalytic conversion rate of 1-butene (black squares) and dimer distribution. (B) Dimer selectivity as a function of the conversion of 1-butene over a 6 wt % Ni-Ca-LTA catalyst. Conditions: T = 160 °C, p = 50 bar, WHSV = 6−245 h^{-1}.

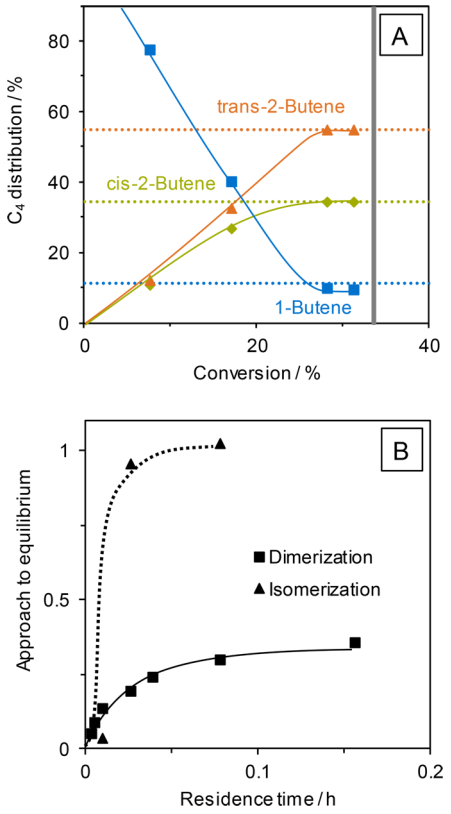

Figure 3. (A) Reactant isomerization behavior over 6 wt % Ni-Ca-LTA. The dotted lines give the equilibrium at 50 bar and 160 °C. (B) Approach to equilibrium for dimerization and isomerization. Reaction conditions: T = 160 °C, p = 50 bar, WHSV = 6−245 h^{-1}.

Figure 3B shows the approach to equilibrium for the two parallel reactions: dimerization and butene double-bond isomerization (defined as the ratio of the different isomers; see the Supporting Information for details). Isomerization increased rapidly to a value of 1 with butene conversion, indicating equilibration, while dimerization did not exceed a value of 0.35 (Figure 3B). Therefore, it is suggested that double-bond isomerization, i.e., the increasing concentration of 2-butene, limits the conversion level.

The dimer selectivity as a function of 1-butene conversion is shown in Figure 2B. Methylheptene and octene were the predominant products of 1-butene dimerization, while dimethylhexene was formed in significantly lower concentrations. The changes in dimer product selectivity and the double-bond isomerization with butene conversion show that octene is formed solely from 1-butene and that dimethylhexene is solely formed from 2-butene dimerization.

Methylheptene can be formed from both 1- and 2-butene. Scheme 1 shows the reaction pathways proposed for the dimerization of 1-butene. The adsorption of the first butene molecule on the Ni active site is hypothesized to take place at the primary (1′-adsorption) or at the secondary carbon atom (2′-adsorption).[20,39−42] The insertion of the second butene for C−C bond formation can also take place at the primary (1′-insertion) or secondary (2′-insertion) carbon. The modes of adsorption and insertion and their probability determine the selectivity to the dimer isomers (octene, 3-methylheptene, and 3,4-dimethylhexene). The obtained product distribution indicates that the main route in dimerization with Ni-Ca-

Scheme 1. Possible Pathway for the Formation of the Dimer Isomers from 1-Butene (Black) and 2-Butene (Green)[a]

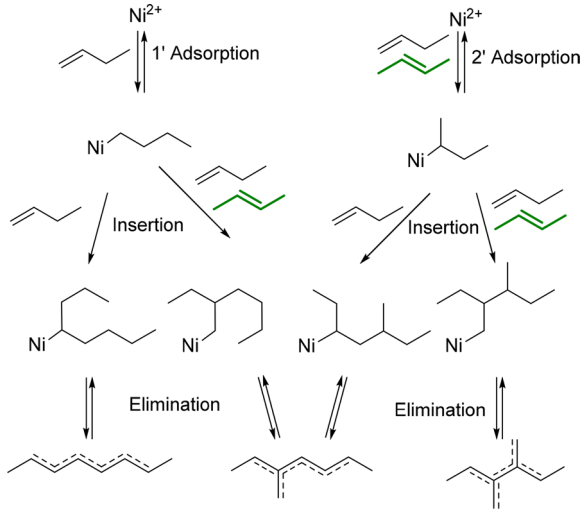

[a]Adapted from the Cossee−Arlman mechanism.[39]

LTA takes place either by 1′-adsorption of 1-butene and 1′-insertion or 2′-insertion of 1-butene, because *n*-octene and methylheptene were formed preferentially.

At higher conversions, the increase in selectivity to methylheptene and dimethylhexene is attributed to a larger contribution of the 2′-adsorption and/or 2′-insertion pathway. This is speculated to be also the result of a higher 2-butene

DOI: 10.1021/acscatal.8b03095
ACS Catal. 2019, 9, 315−324

concentration from the double-bond isomerization of 1-butene (the options for 2-butene are shown in green in Scheme 1). Therefore, octene and methylheptene are concluded to be the primary products and dimethylhexene is a secondary product. It is noted in passing that the absence of BAS is responsible for the low dimethylhexene selectivity. In the presence of BAS, formation of dimethylhexene (selectivity above 30%) is favored by the formation of secondary carbenium ions.[11,28,37,43]

Effect of 2-Butene on the Deactivation of Ni-Ca-LTA. The limiting butene conversion of 35% (leveling off at a rate of 5×10^{-5} $mol_C/(g\ s)$, Figure 2) and chemically equilibrated double-bond isomerization, taken together, suggest that 2-butene hinders further dimer formation (Figure 3). To test this hypothesis, pure *cis*-2-butene was fed and oligomerized (Figure 4). With *cis*-2-butene, rates were significantly lower and

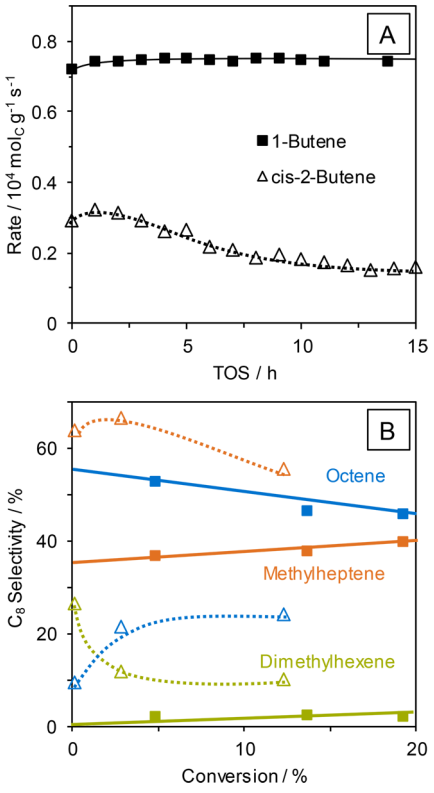

Figure 4. (A) Conversion rate, in terms of the moles of carbon, and (B) product distributions of 1-butene and *cis*-2-butene dimerization reactions over 6 wt % Ni-Ca-LTA at 160 °C, 50 bar, and WHSV = 12.5 h^{-1} (A) and WHSV = 12−245 h^{-1} (B). The conversion of *cis*-2-butene is shown as empty triangles, the reaction of 1-butene is presented as filled squares, as are the corresponding products. Colors of products: *n*-octene (blue), methylheptene (orange), dimethylhexene (green).

decreased much more rapidly (Figure 4A), and also higher selectivities to methylheptene and slightly higher selectivities to dimethylhexene (Figure 4B) were observed. Therefore, following the reaction pathway of Scheme 1, 2-butene can only adsorb via 2′-adsorption (Scheme 1, green), leading to branched products only. The fact that *n*-octene was also formed, even at lower conversions, suggests that a small fraction of 2-butene was isomerized to 1-butene, which in turn acted as a precursor to *n*-octene.

In order to understand the low activity of Ni-Ca-LTA in the dimerization of 2-butenes, the feed was switched between 1- and 2-butene (Figure 5). The first transient from 1-butene to *cis*-2-butene (Figure 5A) led to a rapid decrease in butene

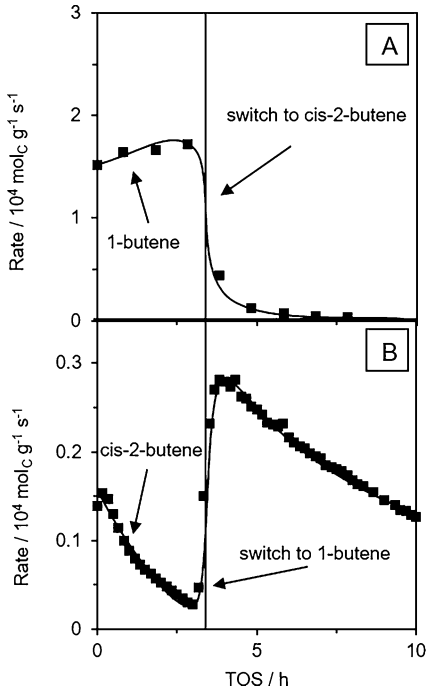

Figure 5. Effect of *cis*-2-butene on butene consumption rate over a 6 wt % Ni-Ca-LTA, at T = 160 °C and P = 50 bar, (A) starting with 1-butene and switching to *cis*-2-butene (WHSV = 50 h^{-1}), and (B) experiment starting with *cis*-2-butene and switching to 1-butene (WHSV = 50 h^{-1}).

conversion rate. In a second experiment, the reactor was first fed with 2-butene and subsequently switched to 1-butene. This transient increased the dimerization activity, but to a level that was approximately 1 order of magnitude lower than that starting from 1-butene (Figure 5B and comparison to Figure 5A). Thus, we conclude that 2-butene induced irreversible changes to the most active sites of Ni-Ca-LTA.

On the basis of the above results, we conclude that 1-butene isomerizes to 2-butene, inducing rapid deactivation, especially at higher conversions. The higher concentration of 2-butene in comparison to 1-butene (90% 2-butene and 10% 1-butene at conversions above 30%, Figure 3A) leads also to an increase in the selectivity to products formed from the 2′-adsorption pathway: i.e., methylheptene and dimethylhexene (Figure 2B). However, the selectivity to *n*-octene is still higher than that to dimethylhexene, indicating a significantly faster dimerization for 1-butene than for 2-butene.

The low activity in 2-butene dimerization is hypothesized to be caused by the formation of a stable Ni-alkyl species either via the 2′-adsorption or via the insertion of another alkene (1-butene or 2-butene) into the secondary carbon of the adsorbed 2-butene. Thus, the deactivation over time observed in Figure 1 is concluded to be caused by the high concentration of 2-butene (ca. two-thirds of butene at 20% butene conversion), leading to the formation of a surface species that is unable to desorb.

To analyze the carbonaceous deposits resulting from exposure to 2-butenes, spent catalysts were dissolved in HF and the remainder was subsequently dried at 90 °C. The organic residue was dissolved in hexane and analyzed by gas

DOI: 10.1021/acscatal.8b03095
ACS Catal. 2019, 9, 315−324

chromatography. A higher concentration of C_{16+} was observed after 2-butene dimerization, while concentrations of hydrocarbons between C_{12} and C_{16+} were similar to those obtained after 1-butene dimerization. This suggests that 2-butene dimerization forms larger oligomers that block and deactivate Ni^{2+} sites.

Kinetics of 1-Butene Dimerization. The reaction orders obtained for the formation of octene and methylheptene (Figure 6), with respect to 1-butene, were approximately 2

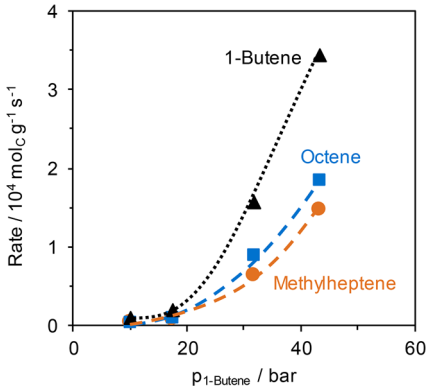

Figure 6. Reaction of 1-butene consumption and formation of methylheptene and octene over 6 wt % Ni-Ca-LTA. Conditions: T = 160 °C, p = 50 bar, WHSV = 15−156 h^{-1}, 1-butene feed mix diluted with propane with $c_{1\text{-butene}}$ = 20−86 wt %.

(Figure S7C,D). This points to the C−C coupling of the two weakly adsorbed butenes as the rate-determining step (rds), in agreement with studies on ethene dimerization.[21,44−46] The measured activation energies for the formation of the specific dimers, as well as for the different oligomers, are shown in Table 1 (Arrhenius plots are shown in Figure S7A,B in the Supporting Information). The reaction order and activation energy were not measured for dimethylhexene, since it is a secondary product. Among the dimers, the values of apparent activation energies (E_a) determined for methylheptene and octene were similar (76 and 72 kJ/mol, respectively) and indicate that both products stem from a pathway with a similar transition state. The values were similar to those obtained by Zhang et al. with Ni-ZSM-5.[47] As previously shown in Scheme 1, the formation of dimethylhexene requires the 2′-adsorption and 2′-insertion of 1-butene or 2-butene. Therefore, prior to the formation of dimethylhexene, isomerization of 1-butene into 2-butene must take place.

Table 1. Energy of Activation for the Butene Consumption as well as for the Formation of Products at Conversion Levels between 0.5 and 3.5%[a]

	E_A (kJ mol^{-1})
C_4 consumption	73
methylheptene formation	76
octene formation	72

[a]Conditions: WHSV = 150 h^{-1}, p = 50 bar, T = 140−180 °C. Arrhenius plots are shown in Figure S7 in the Supporting Information.

IR Spectra of Adsorbed and Reacted Butenes. IR spectroscopy was used to characterize the adsorbed species and monitor the gradual isomerization of adsorbed butenes as the reaction proceeded. The basic nature of the catalysts stabilizes carbonates, which change in nature and concentration during the reaction. We hypothesize that these carbonates are largely spectators to the catalytic transformations. However, their presence will moderate the acid−base properties of the investigated catalysts.

Exposure of the activated zeolites to 1-butene and subsequent evacuation led to IR spectra of adsorbed 1-butene on Ca-LTA and Ni-Ca-LTA that are compiled together with the assignments in SI-5, Table S4, and Figures S8 and S9 in the Supporting Information. The spectra of 1-butene adsorbed on Ca-LTA and Ni-Ca-LTA showed bands at 1300−1700 cm^{-1} (Figure S8), which are characteristic of C=C stretching, C−H bending, and carbonate or carboxylate vibrations. The assignments and the discussion of the carbonate bands are provided in SI-5. The IR spectra of 1-butene adsorption on Ca-LTA and Ni-Ca-LTA in the 2700−3200 cm^{-1} region are shown in Figure S9. Admission of butene leads to C−H stretching bands on both samples. The bands above 3000 cm^{-1} are attributed to C−H stretching vibrations at C=C bonds, while the bands below 3000 cm^{-1} are attributed to C−H vibrations at C−C bonds of physisorbed alkenes.[48,49]

After activation of Ni-Ca-LTA, 1-butene was adsorbed at constant pressure (1 mbar) and IR spectra (Figure 7) showed bands characteristic of bidentate carbonate, as described in SI-5. The most pronounced bands between 1620 and 1660 cm^{-1} are assigned to π-bonded butene on Ni^{2+}. Directly after exposure of the sample to a stream of 1-butene, a band at 1622 cm^{-1} with a shoulder at 1658 cm^{-1} (attributed to gaseous 1-

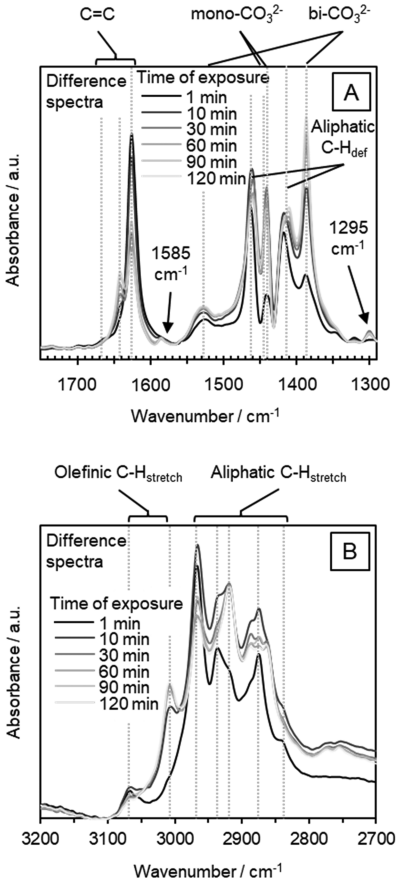

Figure 7. IR spectra of 6 wt % Ni-Ca-LTA at 40 °C exposed to 1 mbar of 1-butene after 1−30 min: (A) 1300−1700 cm^{-1} range; (B) 2700−3200 cm^{-1} range.

DOI: 10.1021/acscatal.8b03095
ACS Catal. 2019, 9, 315−324

butene[50]) was observed. The band at 1622 cm^{-1} was tentatively attributed to π-bonded 1-butene.[48,51,52] After 10 min, a band at 1641 cm^{-1} evolved. It is attributed to an adsorbed alkene with an internal double bond (π-bound 2-butene or a branched octene), since the higher wavenumber indicates a stronger C═C bond for 2-butene in comparison to the external C═C bond observed for 1-butene (1622 cm^{-1}).[50,53] This is further supported by the variations of the relative intensity of the CH vibrations at 1440, 1408, 3061, and 3005 cm^{-1} (Figure 7), indicating an increasing number of ═CH vibrations in the surface species.

The changes observed in the concentration of methyl groups of the adsorbed hydrocarbons allowed us to follow double-bond isomerization and/or dimerization reactions of 1-butene. An increase in the intensity of the CH_3 group vibration (1390 cm^{-1}, Figure 7A), especially within the first 30 min, and in the CH_3 bending vibration (2873 and 2967 cm^{-1}, Figure 7B) suggests that several CH_3 groups were formed, as the combined result of isomerization and alkene addition. Because the intensity of the CH_2 bands (2841 and 2939 cm^{-1}) remained constant throughout the experiment, we conclude that double-bond isomerization and the formation of surface alkyl species are the main surface reactions under these conditions. Within the 30 min of exposure, two additional bands appeared at 1585 and 1295 cm^{-1}. The lower wavenumber is attributed to a delocalized C═C bond stretching vibration, tentatively assigned to π-allyl formation.[54] In addition, the band at 1295 cm^{-1} is assigned to the stretching of a carbenium ion ($\nu_{as}(C^+-C)$).[55−57] The allyl species is hypothesized to lead to isomerization, while the carbenium ion is suggested to be a key intermediate in the dimerization (Scheme 2).

Scheme 2. Surface Intermediates Detected upon Butene Adsorption on Ni-Ca-LTA and Their Proposed Reactivity

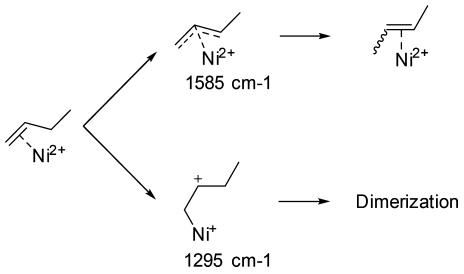

Enthalpic Contribution of Adsorption of Butenes on Ni-Ca-LTA. The heat of adsorption of 1-butene on Ni-Ca-LTA was 63 kJ mol^{-1} (Figure S10). A Langmuir approach was used to fit the isotherm, with a maximum surface coverage of 0.73 $mmol_{1\text{-butene}}/g$ and an adsorption constant K of 4.9×10^{-3} bar^{-1} (SI-6) at 40 °C. This adsorption constant at 40 °C gives an adsorption constant of 6.0×10^{-6} bar^{-1} at 160 °C, according to the van't Hoff equation (SI-6). This adsorption constant translates to Ni^{2+} sites nearly saturated with 1-butene, as predicted by the Langmuir adsorption isotherm ($P_{1\text{-butene}}$ = 42.5 bar). The high adsorption enthalpy of 63 kJ mol^{-1} indicates a strong interaction of the alkene with the Ni, leading to the formation of a Ni alkene complex, potentially increasing the electron density at Ni^{2+}. It should be noted in passing that this hypothesized interaction was not manifested in XANES at the Ni-K edge energy (8333 eV).

The adsorption of 2-butene was also examined (Figure S11). A successive weight increase was observed within the first 12 h at 0.03 mbar of 2-butene. The initial adsorption enthalpy was, however, approximately 63 kJ mol^{-1} and hence similar to that for 1-butene.

Catalytic Pathway of Butene Dimerization on Ni-Ca-LTA. The product distribution and the concluded formation of a Ni-alkyl complex (Scheme 1) are compatible with the proposed dimerization mechanism. The obtained product distribution indicates that the dimerization is mainly taking place by 1′-adsorption of 1-butene and 1′-insertion or 2′-insertion of 1-butene, because *n*-octene and methylheptene were formed preferentially. In contrast, a metallacycle mechanism would involve the formation of the three dimers in comparable concentrations. Their ratio would depend on the adsorption and insertion orientation of the π-bound alkenes.[58,59] The very low formation rates of dimethylhexene and its nonexistence at 0% conversion led us to conclude that the metallacycle mechanism is not operative for Ni-Ca-LTA.

The product distribution obtained on Ni-Ca-LTA points to a stepwise mechanism for butene dimerization. We propose a dimerization pathway adapted from the Cossee−Arlman mechanism (Scheme 3), which involves initially the formation of a Ni-alkyl complex as the active site throughout the entire catalytic cycle (Scheme 3). The full coverage of Ni by 1-butene and the reaction order of 2 with respect to 1-butene support the formation of a Ni-alkyl complex as the active site; this site is able to coordinate to two additional butene molecules that lead to the dimer. The catalytic cycle begins with the adsorption of 1-butene on the Ni-alkyl complex, preceded by

Scheme 3. Proposed Reaction Network for Dimerization of Linear Butenes over Ni Active Sites (Ni-alkyl in the Zeolite)[a]

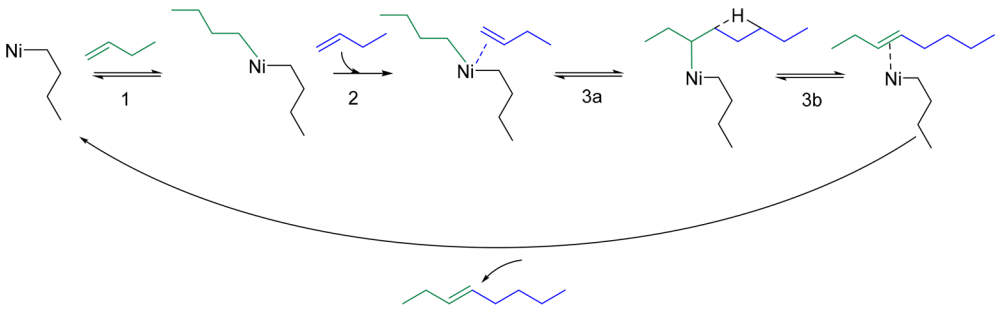

[a]First, 1-butene (green) would adsorb on the Ni-alkyl complex (1). A second butene molecule (blue) weakly adsorbs on the Ni-$alkyl_{C4}$ complex (2). Collectively, dimerization takes place on the Ni-$alkyl_{C8}$ complex (3), this step being rate limiting. Finally, there is a subsequent internal hydride shift, leading to product desorption from the Ni site and formation of the Ni-$alkyl_{C4}$ complex for a new catalytic cycle.

DOI: 10.1021/acscatal.8b03095
ACS Catal. 2019, 9, 315−324

the formation of a covalent bond with the Ni-alkyl complex (step 1, Scheme 3), in chemical equilibrium with the gas-phase butene. We view the allyl complex as the intermediate for the isomerization of π-bonded 1- and 2-butene on Ni (Scheme 2). In the next step, a second butene molecule weakly adsorbs via π-bond interaction. Consecutively, the third step is the kinetically relevant C−C bond formation that forms the C_8 alkene product (step 3 in Scheme 3). Desorption of the C_8 alkene regenerates the Ni-alkyl$_{C4}$ complex, making it ready for the next catalytic cycle. Pseudo-steady-state treatments of the intermediates, together with assumptions of binding sites and the Ni-alkyl complex as the most abundant surface intermediates (step 1, Scheme 3), give the rate expression (derivation given in SI-4),

$$r = \frac{K_1 K_2 k_3 [C_4]^3}{1 + K_1[C_4] + K_2[C_4] + [C_8]/K_4} \approx k[C_4]^2$$

which simplifies to an apparent second-order dependence at low surface coverages in the limit of low product concentration. K and k are the equilibrium constants for adsorption and elementary C−C bond formation of the kinetically relevant step, respectively, as also defined in Scheme 3.

It should be noted that, according to Scheme 3, an internal hydride shift (step 3a) is necessary, before the products can desorb from the Ni site and regenerate the active site to form a new Ni-alkyl complex. Brogaard et al.[20] have estimated that Ni-alkene-alkyl complexes of different alkyl chain lengths are quite close in free energy in the Cossee−Arlman pathway. Similarly, the proposed mechanism suggests a change to a larger adsorbate for the Ni-alkene-alkyl complex, evolving from a Ni-alkene-alkyl$_{C4}$ to a Ni-alkene-alkyl$_{C8}$. The reason for this modified Cossee−Arlman mechanism on Ni-zeolite is attributed to the absence of BAS.[20] The lack of Brønsted acidity also agrees well within the high yields to linear and monobranched C_8 isomers, because dibranched dimers are favored by Brønsted acid catalyzed dimerization.[32,33]

While this is a plausible mechanistic pathway, the strong adsorption of butene on Ni^{2+} and the chemical potential of the reacting butene suggest that the reaction starts from a Ni-alkyl complex. This complex is equivalent to those observed in homogeneous systems,[8] having ligands coordinated to Ni metal that alter the electronic charge of its d orbital. The observed second order and the full coverage requires postulation of the presence of this Ni alkene complex that moderates the coordination of the reacting butenes with Ni^{2+}.

The insertion step defines the product selectivity upon the orientation of the adsorbed butene molecule. The possible orientations of the butene molecules within the cyclic transition state are shown in Scheme S1 in the Supporting Information, as those proposed by theory with Ni homogeneous complexes.[44] In this case a relatively low stability of the primary carbenium ion that would be formed upon a 2′-adsorption of 1-butene is proposed (Scheme S1 B in the Supporting Information). Hence, an initial 1′-adsorption of pure 1-butene is preferred. Once 2-butene is available from the double-bond isomerization of 1-butene, 2′-adsorption of 2-butene leads to a better stabilized secondary carbenium ion, which opens another dimerization pathway via this intermediate. In all cases, however, the butene insertion step is associated with the highest activation barrier.

CONCLUSION

1-Butene dimerization on a Ni-Ca-LTA-derived catalyst was highly selective to methylheptene and *n*-octene (95%), shifting the methylheptene/octene ratio from 0.7 to 1.4, in a conversion range up to 35%. The main dimerization pathway is proposed to take place via initial 1′-adsorption of 1-butene on Ni and subsequent 1- or 2-insertion of a second butene, leading to the high selectivity to methylheptene and *n*-octene dimers.

Double-bond isomerization of butene is also catalyzed by Ni^{2+} in Ni-Ca-LTA. The extent of dimerization plays an important role in the dimerization pathway. High concentrations of 2-butene favor the 2′-insertion into 1′-adsorbed species, increasing the selectivity to methylheptene. The 2′-adsorption is the only possible mode for internal alkenes, causing a high concentration of 2′-adsorbed species and leading to the formation of mono- and dibranched dimers. Double-bond isomerization equilibrium is reached at about 30% conversion and limited the conversion rate to dimers by almost 1 order of magnitude. Adsorbed 2-butene or its dimerization products also lead to irreversible changes at the active sites and block them by the formation of strongly bound oligomers.

IR spectroscopy shows that Ni-allyl and Ni-alkyl complexes are formed as the most abundant intermediates during isomerization and dimerization. During isomerization, the adsorption−desorption is equilibrated and the reactants assume an allylic transition state.

Dimerization of linear butenes on Ni-Ca-LTA follows a Cossee−Arlman type mechanism. After formation of the Ni-alkyl complex, two butene molecules form a C−C bond. Ni sites are interacting with 1-butene, forming Ni-alkyl complexes, at which a second-order kinetically relevant C−C bond formation occurs that leads to octenes. These findings suggest that the Ni^{2+} species which catalyzes the reaction exists in a very special chemical environment involving an additional coordinated butene.

EXPERIMENTAL SECTION

Catalyst Preparation. Ca-LTA was obtained by stirring Ca-LTA-5A (Sigma-Aldrich, precalcined 4 h, rate 5 °C/min, 500 °C) with water (20 $g_{water}/g_{zeolite}$) at 80 °C for 24 h (pH 7−8 over total exchange time). The solid was recovered and washed thoroughly with deionized water. After it was dried at 100 °C for 10 h, the precursor was calcined (8 h, rate 5 °C/min, 500 °C, air). Ni-Ca-LTA with different Ni wt % was prepared by aqueous ion exchange of Ca-LTA-5A with Ni^{2+}. The Ni^{2+} ion exchange was carried out with an aqueous $Ni(NO_3)_2$ (Sigma-Aldrich) solution (20 $g_{solution}/g_{zeolite}$) at 80 °C for 24 h. The molarity of the solution varied between 0.00 and 0.06 M to give 0−6 wt % Ni^{2+} in Ca-LTA (0 wt % of Ni^{2+} was obtained in the case of no $Ni(NO_3)_2$ in solution). During Ni ion exchange, the pH value was 6−7 during the total time of exchange (Figure S12). The charge balance was approximately 100% with respect to Al atoms (Table S5). The solid was recovered and washed thoroughly with deionized water. After it was dried at 100 °C overnight, the precursor was calcined (8 h, rate 5 °C/min, 500 °C, air).

Characterization Methods. Two different methods were followed in the adsorption of 1-butene on Ni-Ca-LTA via IR: 1-butene was adsorbed, equilibrated, and subsequently evacuated stepwise, and the time-resolved adsorption of 1-

DOI: 10.1021/acscatal.8b03095
ACS Catal. 2019, 9, 315−324

butene was carried out at a constant pressure. In the first method, low-pressure IR spectra were recorded on a Vertex 70 spectrometer from Bruker Optics, equipped with a liquid nitrogen cooled detector. A thin and self-supporting wafer was installed and activated for 1 h at 450 °C (rate 10 °C/min) under vacuum. After the system was cooled to 40 °C, butene was adsorbed to 0.5 mbar and then later evacuated ($P < 10^{-7}$ mbar). Scans were taken with a resolution of 0.4 cm^{-1}, with an average of 120 scans per spectrum. In the second approach, for IR spectroscopy at constant pressure, the samples were prepared as self-supporting wafers and first activated under vacuum at 450 °C (rate 10 °C/min) in situ for 2 h. After pretreatment, the activated samples were cooled to 40 °C. Subsequently, 1-butene was adsorbed at 1 mbar. Spectra were recorded after 1−30 min on a Nicolet iS50AEM spectrometer from ThermoScientific, equipped with a liquid nitrogen cooled detector at a resolution of 4 cm^{-1}. Scans were taken from 1000 to 4500 cm^{-1} with an average of 500 scans per spectrum.

For determination of the coke, spent catalysts (24 h on stream at 160 °C and 50 bar, WHSV = 50 h^{-1}) were dissolved in a sufficient amount (~20 mL) of HF at 80 °C. After evaporation of HF, the residue was collected in hexane and injected into a GC equipped with a 50 m HP-1 column and a flame ionization detector.

X-ray diffraction (XRD) measurements were performed in a PANalytical Empyreal System diffractometer, equipped with a Cu Kα radiation source (Kα_1 line of 1.54 Å; 45 kV and 40 mA)). The diffractograms were measured by the usage of a sample spinner stage in a 2θ range between 5 and 70° (step size 0.0131303/2θ) under ambient conditions.

X-ray absorption (XAS) spectra were recorded at DESY in Hamburg, Germany at PETRA III, P65. The monochromatic photon flux was at 2×10^{12} s^{-1} at 9 keV and a beam size of 0.5 × 1 mm^2. The sample was packed in a in situ XAS setup capillary and activated in 10% O_2 under a He flow (5 mL/min) at 450 °C (rate 10 °C/min) for 2 h. After it was cooled to 160 °C, the system was flushed with He. The spectra were recorded between 8160 and 8700 eV and evaluated with Athena software.[60] For the linear combination fit, NiO and Ni foil were applied as standards for Ni^{2+} and Ni^0, respectively.

For the determination of the particle size, the catalyst particles were enhanced (magnification 2000×) by a high-resolution JEOL JSM-7500F scanning electron microscope (voltage 2 kV) and subsequently measured. For the sample preparation a small amount of catalyst was sonicated in EtOH, dropped on the sample Cu grid and dried under ambient conditions.

The gravimetric sorption isotherms of 1-butene and 2-butene on Ni-Ca-LTA were measured with a Setaram TG-DSC 111 thermoanalyzer connected to a high-vacuum system. About 20 mg of sample was placed in a quartz crucible and activated at 450 °C (rate 10 °C/min) for 1 h under vacuum ($p < 10^{-4}$ mbar). After it was cooled to 40 °C, the sample was exposed to 1-butene in small pressure steps from 0.01 to 10 mbar. Both the sample mass and the thermal flux were monitored. The heat of adsorption was directly obtained by integration of the observed heat flux signal. During the adsorption of 2-butene on Ni-Ca-LTA a successive weight increase was observed during the first 12 h at 0.3 mbar of 2-butene. The adsorption enthalpy was directly obtained by integration of the heat flux signal for the same time interval as for 1-butene.

The BET specific surface area and pore volume of the zeolite were determined by nitrogen physisorption. The isotherms were measured at liquid nitrogen temperature (77 K) using a PMI Automatic Sorptometer. The catalyst was activated under vacuum at 473 K for 2 h before measurement. The apparent surface area was calculated by applying the Brunauer−Emmett−Teller (BET) theory with a linear regression in the range p/p_0 = 0.01−0.15. The micro- and mesopores were determined from the t-plot linear regression for t = 5−6 Å.

Catalytic Testing and Reaction Kinetics. Catalytic tests were conducted in a fixed bed plug flow reactor (PFR (i.d. = 3.9 mm)), connected to an online GC analysis unit (Agilent HP 6890, equipped with a 50 m HP-1 column). Prior to GC analysis, hydrogen was added to the product stream, which was hydrogenated over a Pt/Al_2O_3 catalyst. A mixture of 15% isobutane and 85% 1-butene was introduced by a syringe pump (ISCO Model 500 D), the temperature was controlled by a Eurotherm 2416 apparatus, and the pressure was controlled using a Tescom backpressure regulator.

Prior to weighing, the catalyst was dried at 100 °C for 1 h. The catalyst bed was diluted with SiC and fixed in the isothermal zone of the reactor. After activation for 2 h at 450 °C (rate 10 °C/min) in air, the system was purged with nitrogen and pressurized to the desired pressure. Subsequently the system was flushed with the feed mixture (5 mL/min) for 2 min. After the desired flow rate was set, the temperature program and GC measurements were started.

Standard measurement conditions were at 160 °C and 50 bar with a flow rate of the butene mixture between 0.04 and 0.12 mL/min. These reaction conditions resulted in higher activity and lower deactivation. Catalyst loading was varied between 10 and 200 mg. WHSV was in the range 6−244 g g^{-1} h^{-1}.

The activation energy was determined between 140 and 180 °C at 50 bar with a WHSV of 150 h^{-1}. The reaction order was measured at 50 bar total pressure, 160 °C, and WHSV of butene of 25 h^{-1}. The feed was diluted with propane, which led to concentrations of 1-butene between 32 and 86 wt %.

Isobutane is inert under the reaction conditions applied, and hence it was used as an internal standard for normalization of GC areas. Conversion, selectivity, and yield were calculated according to the equations

$$X = \frac{n(\text{butene})_{\text{in}} - n(\text{butene})_{\text{out}}}{n(\text{butene})_{\text{in}}}$$

$$S = \frac{n(\text{product})_{\text{out}}}{n(\text{butene})_{\text{in}} - n(\text{butene})_{\text{out}}} \frac{|\nu_{\text{butene}}|}{\nu_{\text{product}}}$$

$$Y = \frac{n(\text{product})_{\text{out}}}{n(\text{butene})_{\text{in}}} \frac{|\nu_{\text{butene}}|}{\nu_{\text{product}}}$$

■ ASSOCIATED CONTENT

Supporting Information

The Supporting Information is available free of charge on the ACS Publications website at DOI: 10.1021/acscatal.8b03095.

Additional graphs, experimental details, characterization data, thermodynamic equilibrium data, considerations on approach to equilibrium and reaction kinetics, and additional reaction schemes (PDF)

DOI: 10.1021/acscatal.8b03095
ACS Catal. 2019, 9, 315−324

AUTHOR INFORMATION

Corresponding Authors

*E-mail for M.S.-S.: m.sanchez@tum.de.
*E-mail for R.B.-D.: ricardo.bermejo@tum.de.
*E-mail for J.L.: johannes.lercher@tum.de.

ORCID

Yue Liu: 0000-0001-8939-0233
Andreas Jentys: 0000-0001-5877-5042
Ya-Huei Cathy Chin: 0000-0003-3402-4097
Johannes Lercher: 0000-0002-2495-1404

Notes

The authors declare no competing financial interest.

ACKNOWLEDGMENTS

This work was funded by EVONIK Performance Materials GmbH. J.L. acknowledges support for this contribution by the U.S. Department of Energy (DOE) (CN 269409), Office of Science, Office of Basic Energy Sciences, Division of Chemical Sciences, Geosciences & Biosciences, for exploring transition metal cations for C−C bond forming reactions. R.B.-D. acknowledges the Alexander von Humboldt foundation for financial support.

ABBREVIATIONS

Al, aluminum; Å, angström; BAS, Brønsted acid sites; BET, Brunauer−Emmett−Teller; C_4, butenes; C_8, octenes; C_{12}, dodecenes; C_{16}, hexadecenes; Ca, calcium; Ca-LTA, Ca-containing LTA; Ca-LTA-5A, commercial zeolite 5 A; Cu, copper; E_a, energy of activation; EtOH, ethanol; eV, electronvolts; GC, gas chromatograph; G, gram catalyst; h, hour; HF, hydrogen fluoride; IR, infrared; k_{di}, rate constant for dimerization; k_{tri}, rate constant for trimerization; LTA, Linde type A zeolite; mA, milliampere; min, minutes; mL, milliliter; mol_C, mols on carbon basis; N_2, nitrogen; Ni, nickel; $Ni(NO_3)_2$, nickel nitrate; Ni-Ca-LTA, nickel-exchanged Ca-LTA; *p*, pressure; pH, pH value; Pt, platinum; Al_2O_3, aluminum oxide; *S*, selectivity; SEM, scanning electron microscopy; Si, silicon; SiC, silicon carbide; *T*, temperature; TGA, thermogravimetric analysis; TOF, turnover frequency; TOS, time on stream; WHSV, w8 hly space velocity; wt %, weight %; *X*, conversion; XANES, X-ray absorption near edge structure; XAS, X-ray absorption spectroscopy; XRD, X-ray diffraction; *Y*, yield

REFERENCES

(1) Weissermel, K.; Hans-Jürgen, A. *Industrial Organic Chemistry*; Wiley-VCH: Weinheim, 1997.
(2) Albrecht, S.; Kießling, D.; Wendt, G.; Maschmeyer, D.; Nierlich, F. Oligomerisierung von n-Butenen. *Chem. Ing. Tech.* **2005**, *77*, 695−709.
(3) Hassan, S. M.; Panchenkov, G. M.; Kuznetsov, O. I. Studies on the Mechanism and Kinetics of Propylene Oligomerization and Hydrooligomerization on Zeolites. *Bull. Chem. Soc. Jpn.* **1977**, *50*, 2597−2601.
(4) Ng, F. T. T.; Creaser, D. C. Ethylene Dimerization over Modified Nickel Exchanged Y-Zeolite. *Appl. Catal., A* **1994**, *119*, 327−339.
(5) Nkosi, B.; Ng, F. T. T.; Rempel, G. L. The Oligomerization of 1-Butene Using NaY Zeolite Ion-Exchanged with Different Nickel Precursor Salts. *Appl. Catal., A* **1997**, *161*, 153−166.
(6) Nkosi, B.; Ng, F. T. T.; Rempel, G. L. The Oligomerization of Butenes with Partially Alkali Exchanged NiNaY Zeolite Catalysts. *Appl. Catal., A* **1997**, *158*, 225−241.
(7) Schultz, R. G.; Engelbrecht, R. M.; Moore, R. N.; Wolford, L. T. Olefin Dimerization over Cobalt-Oxide-on-Carbon Catalysts: II. Butene and Hexene Dimerization. *J. Catal.* **1966**, *6*, 419−424.
(8) Skupinska, J. Oligomerization of α-Olefins to Higher Oligomers. *Chem. Rev.* **1991**, *91*, 613−648.
(9) Fischer, K.; Jonas, K.; Misbach, P.; Stabba, R.; Wilke, G. Zum "Nickel-Effekt". *Angew. Chem.* **1973**, *85*, 1001−1012.
(10) Ziegler, K.; Holzkamp, E.; Breil, H.; Martin, H. Das Mülheimer Normaldruck-Polyäthylen-Verfahren. *Angew. Chem.* **1955**, *67*, 541−547.
(11) Brückner, A.; Bentrup, U.; Zanthoff, H.; Maschmeyer, D. The Role of Different Ni Sites in Supported Nickel Catalysts for Butene Dimerization under Industry-Like Conditions. *J. Catal.* **2009**, *266*, 120−128.
(12) Kumar, N.; Mäki-Arvela, P.; Yläsalmi, T.; Villegas, J.; Heikkilä, T.; Leino, A. R.; Kordás, K.; Salmi, T.; Yu Murzin, D. Dimerization of 1-Butene in Liquid Phase Reaction: Influence of Structure, Pore Size and Acidity of Beta Zeolite and MCM-41 Mesoporous Material. *Microporous Mesoporous Mater.* **2012**, *147*, 127−134.
(13) Mlinar, A. N.; Baur, G. B.; Bong, G. G.; Getsoian, A. B.; Bell, A. T. Propene oligomerization over Ni-exchanged Na-X zeolites. *J. Catal.* **2012**, *296*, 156−164.
(14) Wendt, G.; Kießling, D. Dimerisierung von n-Butenen an Nickelalumosilicat-Katalysatoren. *Chem. Technol. (Leipzig)* **1995**, *3*, 136−143.
(15) Deimund, M. A.; Labinger, J.; Davis, M. E. Nickel-Exchanged Zincosilicate Catalysts for the Oligomerization of Propylene. *ACS Catal.* **2014**, *4*, 4189−4195.
(16) Canivet, J.; Aguado, S.; Schuurman, Y.; Farrusseng, D. MOF-Supported Selective Ethylene Dimerization Single-Site Catalysts through One-Pot Postsynthetic Modification. *J. Am. Chem. Soc.* **2013**, *135*, 4195−4198.
(17) Madrahimov, S. T.; Gallagher, J. R.; Zhang, G.; Meinhart, Z.; Garibay, S. J.; Delferro, M.; Miller, J. T.; Farha, O. K.; Hupp, J. T.; Nguyen, S. T. Gas-Phase Dimerization of Ethylene under Mild Conditions Catalyzed by MOF Materials Containing (bpy)NiII Complexes. *ACS Catal.* **2015**, *5*, 6713−6718.
(18) Metzger, E. D.; Brozek, C. K.; Comito, R. J.; Dincă, M. Selective Dimerization of Ethylene to 1-Butene with a Porous Catalyst. *ACS Cent. Sci.* **2016**, *2*, 148−153.
(19) Mlinar, A. N.; Keitz, B. K.; Gygi, D.; Bloch, E. D.; Long, J. R.; Bell, A. T. Selective Propene Oligomerization with Nickel(II)-Based Metal−Organic Frameworks. *ACS Catal.* **2014**, *4*, 717−721.
(20) Brogaard, R. Y.; Olsbye, U. Ethene Oligomerization in Ni-Containing Zeolites: Theoretical Discrimination of Reaction Mechanisms. *ACS Catal.* **2016**, *6*, 1205−1214.
(21) Agirrezabal-Telleria, I.; Iglesia, E. Stabilization of Active, Selective, and Regenerable Ni-Based Dimerization Catalysts by Condensation of Ethene within Ordered Mesopores. *J. Catal.* **2017**, *352*, 505−514.
(22) Andrei, R. D.; Popa, M. I.; Fajula, F.; Hulea, V. Heterogeneous Oligomerization of Ethylene over Highly Active and Stable Ni-AlSBA-15 Mesoporous Catalysts. *J. Catal.* **2015**, *323*, 76−84.
(23) Beucher, R.; Andrei, R. D.; Cammarano, C.; Galarneau, A.; Fajula, F.; Hulea, V. Selective Production of Propylene and 1-Butene from Ethylene by Catalytic Cascade Reactions. *ACS Catal.* **2018**, *8*, 3636−3640.
(24) Finiels, A.; Fajula, F.; Hulea, V. Nickel-Based Solid Catalysts for Ethylene Oligomerization - A Review. *Catal. Sci. Technol.* **2014**, *4*, 2412−2426.
(25) Moussa, S.; Arribas, M. A.; Concepción, P.; Martínez, A. Heterogeneous Oligomerization of Ethylene to Liquids on Bifunctional Ni-Based Catalysts: The Influence of Support Properties on Nickel Speciation and Catalytic Performance. *Catal. Today* **2016**, *277*, 78−88.
(26) Moussa, S.; Concepción, P.; Arribas, M. A.; Martínez, A. Nature of Active Nickel Sites and Initiation Mechanism for Ethylene Oligomerization on Heterogeneous Ni-beta Catalysts. *ACS Catal.* **2018**, *8*, 3903−3912.

DOI: 10.1021/acscatal.8b03095
ACS Catal. 2019, 9, 315−324

(27) Heveling, J.; Nicolaides, C. P.; Scurrell, M. S. Activity and Selectivity of Nickel-Exchanged Silica-Alumina Catalysts for the Oligomerization of Propene and 1-Butene into Distillate-Range Products. *Appl. Catal., A* **2003**, *248*, 239−248.
(28) Beltrame, P.; Forni, L.; Talamini, A.; Zuretti, G. Dimerization of 1-Butene over Nickel Zeolitic Catalysts: A Search for Linear Dimers. *Appl. Catal., A* **1994**, *110*, 39−48.
(29) Cai, T. Studies of a New Alkene Oligomerization Catalyst Derived from Nickel Sulfate. *Catal. Today* **1999**, *51*, 153−160.
(30) Sarazen, M. L.; Doskocil, E.; Iglesia, E. Catalysis on Solid Acids: Mechanism and Catalyst Descriptors in Oligomerization Reactions of Light Alkenes. *J. Catal.* **2016**, *344*, 553−569.
(31) Sarazen, M. L.; Doskocil, E.; Iglesia, E. Effects of Void Environment and Acid Strength on Alkene Oligomerization Selectivity. *ACS Catal.* **2016**, *6*, 7059−7070.
(32) Sarazen, M. L.; Iglesia, E. Stability of Bound Species During Alkene Reactions on Solid Acids. *Proc. Natl. Acad. Sci. U. S. A.* **2017**, *114*, E3900−E3908.
(33) Sarazen, M. L.; Iglesia, E. Experimental and Theoretical Assessment of the Mechanism of Hydrogen Transfer in Alkane-Alkene Coupling on Solid Acids. *J. Catal.* **2017**, *354*, 287−298.
(34) Takeuchi, D.; Osakada, K. In *Organometallic Reactions and Polymerization*; Osakada, K., Ed.; Springer Berlin Heidelberg: Berlin, Heidelberg, 2014; pp 169−215.
(35) Gal, I. J.; Jankovic, O.; Malcic, S.; Radovanov, P.; Todorovic, M. Ion-Exchange Equilibria of Synthetic 4A Zeolite with Ni2+, Co2+, Cd2+ and Zn2+ Ions. *Trans. Faraday Soc.* **1971**, *67*, 999−1008.
(36) Amari, D.; Ginoux, J.-L.; Bonnetain, L. Textural Damage of Cation-Exchanged LTA Zeolites Studied by Gas Adsorption. *Zeolites* **1994**, *14*, 58−64.
(37) Rabeah, J.; Radnik, J.; Briois, V.; Maschmeyer, D.; Stochniol, G.; Peitz, S.; Reeker, H.; La Fontaine, C.; Brückner, A. Tracing Active Sites in Supported Ni Catalysts during Butene Oligomerization by Operando Spectroscopy under Pressure. *ACS Catal.* **2016**, *6*, 8224−8228.
(38) Mlinar, A. N.; Shylesh, S.; Ho, O. C.; Bell, A. T. Propene Oligomerization Using Alkali Metal- and Nickel-Exchanged Mesoporous Aluminosilicate Catalysts. *ACS Catal.* **2014**, *4*, 337−343.
(39) Cossee, P. Ziegler-Natta Catalysis I. Mechanism of Polymerization of α-Olefins with Ziegler-Natta Catalysts. *J. Catal.* **1964**, *3*, 80−88.
(40) Henry, R.; Komurcu, M.; Ganjkhanlou, Y.; Brogaard, R. Y.; Lu, L.; Jens, K.-J.; Berlier, G.; Olsbye, U. Ethene Oligomerization on Nickel Microporous and Mesoporous-Supported Catalysts: Investigation of the Active Sites. *Catal. Today* **2018**, *299*, 154−163.
(41) Mlinar, A. N.; Ho, O. C.; Bong, G. G.; Bell, A. T. The Effect of Noncatalytic Cations on the Activity and Selectivity of Nickel-Exchanged X Zeolites for Propene Oligomerization. *ChemCatChem* **2013**, *5*, 3139−3147.
(42) Small, B. L.; Schmidt, R. Comparative Dimerization of 1-Butene with a Variety of Metal Catalysts, and the Investigation of a New Catalyst for C□H Bond Activation. *Chem. - Eur. J.* **2004**, *10*, 1014−1020.
(43) Nadolny, F.; Hannebauer, B.; Alscher, F.; Peitz, S.; Reschetilowski, W.; Franke, R. Experimental and Theoretical Investigation of Heterogeneous Catalyzed Oligomerization of a Mixed C4 Stream over Modified Amorphous Aluminosilicates. *J. Catal.* **2018**, *367*, 81−94.
(44) Nikiforidis, I.; Görling, A.; Hieringer, W. On the Regioselectivity of the Insertion Step in Nickel Complex Catalyzed Dimerization of Butene: A Density-Functional Study. *J. Mol. Catal. A: Chem.* **2011**, *341*, 63−70.
(45) Hojabri, F. Dimerisation and Double-Bond Isomerisation of Olefins with a Homogeneous Nickel II-Complex as Catalyst. *J. Appl. Chem. Biotechnol.* **1971**, *21*, 90−91.
(46) Onsager, O.-T.; Wang, H.; Blindheim, U. Niederdruck-Oligomerisation von Mono-Olefinen mit löslichen Nickel/Aluminium-Bimetallkatalysatoren Teil III. Reaktionskinetische Untersuchungen über die Dimerisation und Trimerisation des Áthylens. *Helv. Chim. Acta* **1969**, *52*, 215−223.
(47) Zhang, X.; Zhong, J.; Wang, J.; Zhang, L.; Gao, J.; Liu, A. Catalytic Performance and Characterization of Ni-Doped HZSM-5 Catalysts for Selective Trimerization of n-Butene. *Fuel Process. Technol.* **2009**, *90*, 863−870.
(48) Eberly, P. E., Jr High-Temperature Infrared Spectroscopy of Olefins Adsorbed on Faujasites. *J. Phys. Chem.* **1967**, *71*, 1717−1722.
(49) Socrates, G. *Infrared and Raman characteristic group frequencies: tables and charts*; Wiley: 2001.
(50) Coblentz Society, I. In *NIST Chemistry WEbBook, NIST Standard Reference Database Number 69*; Linstrom, P. J., Mallard, W. G., Eds.; National Institute of Standards and Technology: Gaithersburg, MD 20899, 2017.
(51) Armaroli, T.; Finocchio, E.; Busca, G.; Rossini, S. A FT-IR Study of the Adsorption of C5 Olefinic Compounds on NaX Zeolite. *Vib. Spectrosc.* **1999**, *20*, 85−94.
(52) Kondo, J. N.; Liqun, S.; Wakabayashi, F.; Domen, K. IR Study of Adsorption and Reaction of 1-Butene on H-ZSM-5. *Catal. Lett.* **1997**, *47*, 129−133.
(53) Larkin, P. J. *Infrared and Raman Spectroscopy - Principles and Spectral Interpretation*; Elsevier: 2011.
(54) Chang, C. C.; Conner, W.; Kokes, R. Butene Isomerization over Zinc Oxide and Chromia. *J. Phys. Chem.* **1973**, *77*, 1957−1964.
(55) Olah, G. A.; Baker, E. B.; Evans, J. C.; Tolgyesi, W. S.; McIntyre, J. S.; Bastien, I. J. Stable Carbonium Ions. V.1a Alkylcarbonium Hexafluoroantimonates. *J. Am. Chem. Soc.* **1964**, *86*, 1360−1373.
(56) Olah, G. A.; DeMember, J. R.; Commeyras, A.; Bribes, J. L. Stable Carbonium Ions. LXXXV. Laser Raman and Infrared Spectroscopic Study of Alkylcarbonium Ions. *J. Am. Chem. Soc.* **1971**, *93*, 459−463.
(57) Stepanov, A. G.; Luzgin, M. V.; Romannikov, V. N.; Sidelnikov, V. N.; Paukshtis, E. A. The Nature, Structure, and Composition of Adsorbed Hydrocarbon Products of Ambient Temperature Oligomerization of Ethylene on Acidic Zeolite H-ZSM-5. *J. Catal.* **1998**, *178*, 466−477.
(58) Forestière, A.; Olivier-Bourbigou, H.; Saussine, L. Oligomerization of Monoolefins by Homogeneous Catalysts. *Oil Gas Sci. Technol.* **2009**, *64*, 649−667.
(59) Pillai, S. M.; Ravindranathan, M.; Sivaram, S. Dimerization of Ethylene and Propylene Catalyzed by Transition-Metal Complexes. *Chem. Rev.* **1986**, *86*, 353−399.
(60) Ravel, B.; Newville, M. ATHENA, ARTEMIS, HEPHAESTUS: Data Analysis for X-Ray Absorption Spectroscopy Using IFEFFIT. *J. Synchrotron Radiat.* **2005**, *12*, 537−541.

DOI: 10.1021/acscatal.8b03095
ACS Catal. 2019, 9, 315−324